



ZERO-ORDER OPTIMIZATION BASED SEISMIC DESIGN OF NONLINEAR STEEL MRFs WITH NONLINEAR VISCOUS DAMPERS

O. Idels⁽¹⁾, O. Lavan⁽²⁾

⁽¹⁾ Ph.D. candidate, Faculty of Civil and Environmental Engineering, Technion – Israel Institute of Technology, Technion City, Haifa, Israel, ohadidels@campus.technion.ac.il

⁽²⁾ Associate professor, Faculty of Civil and Environmental Engineering, Technion – Israel Institute of Technology, Technion City, Haifa, Israel, lavan@technion.ac.il

Abstract

Fluid viscous dampers (FVDs) are well-known as one of the predominant damping devices to reduce structural responses and, as a result, structural and nonstructural damage. In the literature many of works successfully integrated the FVDs in moment resisting frame (MRF) structures. Furthermore, some works even utilized optimization approaches to achieve efficient design from both economical and performance point of view. However, most of the research focused on the retrofitting of existing structures. This is due to the fact that FVDs efficiently reduce displacement responses while only slightly increasing, or sometimes even reducing, forces on existing structural elements and foundations. This is very important in retrofitting projects as it reduces the local intervention required. It has been believed that, due to their high cost compared to steel, the use of FVDs in new buildings would not be economic. This misconception may be due to the fact that not the whole design space has been explored.

In the retrofitting optimization problem, the MRF properties are given. The design variables in such problems represent the locations and properties of the FVDs only. In the research to be presented herein, an optimization-based methodology for the design of new nonlinear steel MRFs with nonlinear FVDs is presented. The design variables represent the locations and properties of the FVDs along with the cross-section properties of the elements of the MRF. Taking the properties of both the FVDs and the structural elements enables to explore the whole design space with no parameters set a-priori. This enables reaching non-trivial and non-intuitive designs, while really examining the efficiency of using heavier sections versus adding more damping. Nonetheless, this makes the optimization problem much harder to solve.

The optimization problem formulation relies on a nonlinear time history analysis to evaluate the structural response. The model considers a spread plasticity beam element accounting for moment-axial interaction. A Maxwell model is used to describe the behavior of the nonlinear damper and supporting brace assembly. The cost of the structural elements and FVDs is minimized while the inter-story drifts are constrained to allowable values under various levels of seismicities. The problem is solved using Genetic Algorithms (GA). The results show that, in contrast to what has been believed, the optimized designs are far from relying mainly on the stiffness and strength of the MRF. In fact, the addition of dampers enables a large reduction in the volume of steel elements while satisfying the inter-story drifts constraints. Thus, even though the cost of dampers is high, the total cost of the system considerably reduces.

Keywords: seismic design; fluid viscous dampers; steel moment resisting frames; optimization-based design.



1. Introduction

Moment resisting frames (MRFs) are one of the common lateral load resisting systems. They are widely used and known due to their adequate energy dissipation. In the case of a well-designed MRF, the energy is absorbed in the beam ends due to the development of plastic hinges. Therefore, MRFs may behave well even when subjected to strong ground motions. However, the resulted plastic deformations are in fact structural damage and in many cases would require rehabilitation. Moreover, large deformations are expected due to the plastic hinges, in particular, inter-story drifts, which are also strongly correlated to damage of nonstructural components.

One of the predominant devices to achieve a high-performance level are fluid viscous dampers (FVDs). FVDs reduce the structural response and as a result the damage to structural and nonstructural elements as well as cutting the economic loss. Furthermore, using FVDs within MRFs may be helpful in obtaining a high-performance level. FVDs are very reliable and have been used in military applications for decades, moreover, they are popular for seismic applications. On the other hand, the main disadvantage of FVDs is the relatively high cost compared to MRF elements. To overcome the high price of FVDs and still attain the desired performance level, innovative design strategies have been developed. Among them, even formal optimization frameworks were utilized, where the aim in these works is minimizing the cost while performance constraints are set or vice versa.

In the literature, a large number of studies have investigated the problem of optimal design of MRFs subjected to seismic loads. Some works considered the optimal design problem of MRFs without any supplemental damping devices. In this case, the design variables represent the cross-sections properties. The first paper to consider the PBD philosophy, as a part of the optimization process, was presented by Ganzerli et al. 2000 [1]. In [1], a nonlinear static pushover analysis was adopted while constraining plastic rotations to an allowable value. The pushover analysis has also been adopted in a number of works [e.g. 2, 3] due to the ability to evaluate the structural response beyond the linear region. A more computationally demanding but also a precise method to assess the structural response is the nonlinear response history analysis (NRHA), which has been employed [4,5]. With regard to the optimization problem, the most common approach is to utilize heuristic optimization methods, mainly, Genetic Algorithm (GA) [6–8].

The design of MRFs with FVDs has also been under the spotlight and widely investigated. However, the vast majority of studies focused on the retrofitting design problem for a given MRF with predefined cross-sections properties. In these studies, the design variables represent the locations of the dampers, the damping coefficient or even simultaneously design of both the locations and the coefficients. Some works considered the damping coefficients of the FVDs as continuous design variables [9–12] while others selected the dampers properties out of a predetermined set [12, 13, 14].

Few works focused on the simultaneous design of FVDs and MRF properties. Viti et al. 2006 [16], have considered a hospital retrofitting problem through pushover analysis and Monte Carlo simulation. Takewaki 1999 [17] and Cimellaro 2007 [18], both controlled the amplitudes of the transfer function to achieve efficient distribution of stiffness and damping in shear frames. Lavan et al. 2008 [19] presented a noniterative optimization procedure for nonlinear structures while Lavan 2015 [20] presented a practical design process that relies only on analysis tools.

The design of both the elements and dampers properties have significant importance due to the interaction between the systems. The large forces developed by the dampers have an impact on the element's inherent forces, in particular on the axial forces at the columns. Therefore, simultaneous design, where larger design space is explored may lead to a more efficient design.



In this paper, an innovative framework for the design of the MRF and the FVDs is presented. The methodology relies on NRHA to properly evaluate the dynamic response of the MRF when subjected to deterministic ground record. A spread plasticity beam element is adopted. While the Maxwell model is utilized for the FVDs. GA is used to minimize the total cost of FVDs and the structural elements while satisfying the performance constraints and the code requirements.

2. Governing Equations and NRHA Solution Scheme

In this section, the equations that govern the structural response are presented. We first describe the governing equations of a nonlinear FVDs with an extended brace and a spread plasticity beam model. Then, the equations of motion for a nonlinear frame structure equipped with nonlinear dampers are presented. In this paper MRFs subjected to deterministic ground motion are considered. The framework presented herein relies on nonlinear response history analysis (NRHA), therefore, the analysis properly describe the structural response.

2.1 Damper-brace element model

The damper-brace element utilized in this work considered both the stiffness of the damper and the extended brace. The dashpot accounts for the damping property, as the damping coefficient (c_d) and the exponent α that control the nonlinear behavior. The damper-brace element can be considered as a spring and a dashpot in a series, known also as the Maxwell model. The described element is schematically shown in Fig. 1.

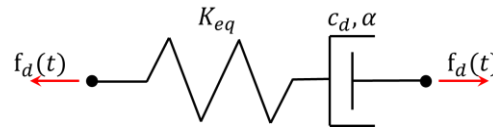


Fig. 1 – Maxwell model

where K_{eq} is the equivalent stiffness of the damper and the extended brace.

The mathematical formulation of this element is given as a first-order differential equation in the following form:

$$\dot{f}_d(t) = k_{eq} \left(\dot{u}_d(t) - \text{sgn}(f_d(t)) \left(\frac{|f_d(t)|}{c_d} \right)^{1/\alpha} \right) \quad (1)$$

where $f_d(t)$ is the resisting forces of the dampers as function of time, $\dot{u}_d(t)$ is the velocity between the element end in local coordinates and $\text{sgn}(\cdot)$ is the sign function in MATLAB.

In order to solve Equation (1) and evaluate the forces at the damper ends at each time step, the fourth-order explicit Runge-Kutta method is utilized, as suggested by [21].

2.2 Spread plasticity beam element

The spread plasticity beam element presented by Spacone et al. 1992 [22] is adopted. This element relies on several integration points and the Gauss-Lobato numerical integration scheme is utilized to evaluate the beam ends rotation based on the curvature at each control section. For example, a beam with three control sections shown in Fig. 2. The moment-curvature relation in every control section is determinant based on the smooth hysteretic rule, as suggested by Sivaselvan and Reinhorn, 2000 [23]. This rule is described in differential form as follows:

$$\dot{M}_h^k = \left\{ aEI_h + (1-a)EI_h \left[1 - 0.5 \left| \frac{M_h^{k,*}}{M_{y,h}^*} \right| \left(\text{sgn}(\dot{M}_h^{k,*} \dot{\chi}_h^k) + 1 \right) \right] \right\} \dot{\chi}_h^k \quad (2)$$

where



$$M_h^{k,*} = M_h^k - aEI_h\chi_h^k \quad ; \quad M_{y,h}^* = (1 - a)M_{y,h} \quad (3)$$

The moment-curvature relation given in Eq. (2) refers to a typical control section k of element h . \dot{M}_h^k and $\dot{\chi}_h^k$ are the time derivatives of the moment and curvature, respectively. The flexural stiffness in the elastic range of every element is denoted by EI_h . The ratio between the post yielding stiffness and the elastic stiffness is denoted by a . $M_{y,h}$ is the yielding moment of the element whereas, $M_h^{k,*}$ is the moment in the hysteretic spring and $M_{y,h}^*$ denotes the yielding moment of the hysteretic spring.

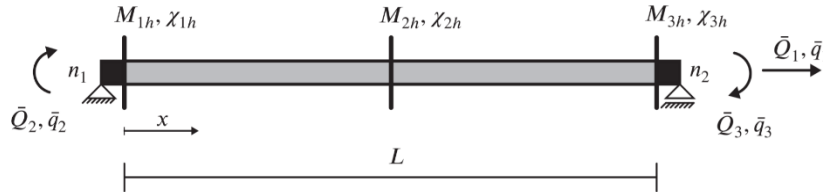


Fig. 2 – beam element with three integration points (sections), Pollini *et al.* 2018

Both the yielding moment and the hysteretic yielding moment are influenced by the axial force. Considering the axial force interaction in a typical element h , the yielding moment is given by Eq. (4). The yielding moment in element h at time step i depends on the axial force from the previous time step $\bar{Q}_{a,i-1}^h$.

$$M_{y,i}^h = \left| -\frac{M_{pl}^h}{N_{pl}^h} |\bar{Q}_{a,i-1}^h| + M_{pl}^h \right| \quad (4)$$

where $M_{pl} = Wf_y$, $N_{pl} = Af_y$. W is the plastic modulus, f_y is the yield stress, A and I are the cross-section's area and moment of inertia, respectively. The cross-section properties and the plastic modulus are responsible for both the stiffness and the strength of the structure. In fact, any change in one of these parameters may lead to better structural performance.

2.3 Equations of motion

In the proposed work we consider a nonlinear plane frame subjected to deterministic ground record. The structural response is evaluated based on the solution of the equations of motion, as given by Eq.(5).

$$\begin{aligned} \mathbf{M}\ddot{\mathbf{u}}(t) + \mathbf{C}_s\dot{\mathbf{u}}(t) + \mathbf{f}_s(t) + \mathbf{f}_d(t) &= -\mathbf{M}\mathbf{e}a_g(t) \\ \mathbf{f}_s(0) &= \mathbf{f}_{s,static} \quad ; \quad \mathbf{f}_d(0) = \mathbf{0} \quad ; \quad \mathbf{u}(0) = \mathbf{u}_{static} \quad ; \quad \dot{\mathbf{u}}(0) = \mathbf{0} \end{aligned} \quad (5)$$

where \mathbf{M} is the mass matrix; \mathbf{C}_s is the Rayleigh inherent damping matrix; \mathbf{f}_s and \mathbf{f}_d are the vectors of restoring forces of the structural elements and dampers respectively; $\mathbf{u}(t)$, $\dot{\mathbf{u}}(t)$ and $\ddot{\mathbf{u}}(t)$ are the displacement, velocity and acceleration at the degrees of freedom in relation to the ground as a function of time, t , respectively; \mathbf{e} is the influence vector; $a_g(t)$ is a vector of the ground motion acceleration over time. While $\mathbf{f}_{s,static}$ and \mathbf{u}_{static} are the vectors of structural elements resisting forces and displacements under gravity loads, respectively.

To conclude this section, the solution scheme presented by Pollini *et al.* 2018 [24] has been adopted, with some modifications. The modifications include the geometrical nonlinearity, known as the second-order effects ($P - \Delta$) by negative stiffness matrix [25]. The analysis also accounts for a uniform distributed load on the beam elements. For the time stepping, we utilized the Newmark-beta integration scheme, while the Newton-Raphson algorithm is applied to achieve equilibrium in each time step.



3. Optimization Problem Formulation

In this section, an optimization problem for the simultaneous design of both the frame and the nonlinear FVDs properties is formulated. The goal of the optimization is to minimize the combined cost of the FVDs and the elements while performance and code constraints are being satisfied to the desired level. The design variables of the optimization problem are the cross-section properties of each type of element in the structure, which are selected out of standard steel table (e.g. IPE, HEB) and the FVDs properties.

3.1 Design variables

As mention above, the design variables represent the cross-section and the FVDs properties. To achieve a practical design that can be easily implemented, the cross-sections are optimally selected from a predefined standard set. The cross-section properties, which affect the structural response, are the moment of inertia (I), the area (A) and the plastic modulus (W). However, if standard steel tables are used, it is possible to represent all the properties of the cross-section by just one parameter [26]. Accordingly, in this paper, the cross-section properties are represented by the plastic modulus (W). Therefore, the design variables of the frame elements can be defined as follows:

$$W_i \in \{W_1 ; W_2 ; W_3 ; W_4 ; \dots\} \quad (6)$$

where W_i is the plastic modulus of the i^{th} element, selected out of a predefined table.

The dampers can be assembled in predefined locations, to attain practical design, for each potential location there are only three possible states: no damper; damper from group one; damper from group two. The dampers are divided into groups based on their mechanical properties, in this work, the groups are characterized by the same damping coefficient (c_d). The design variables related to the j^{th} damper ($c_{d,j}$) are defined as follows:

$$c_{d,j} \in \{0 ; \bar{C}_d \cdot y_1 ; \bar{C}_d \cdot y_2\} \quad (7)$$

where \bar{C}_d represents the maximum damping coefficient available, and it is defined as a priori. y_1 and y_2 are continuous design variables defined in the interval of $[0, 1]$ and scales the maximum available damping coefficient \bar{C}_d of groups one and two, respectively.

3.2 Cost function

The total cost (J) of a MRF equipped with FVDs is evaluated based on two major components, the total cost of steel in the frame (J_{str}) and the total cost of FVDs (J_{damp}), as given in Eq. (8).

$$J = J_{str} + J_{damp} \quad (8)$$

The total cost of steel in the frame (J_{str}) is estimated based on the total volume of steel multiplied by the cost of steel per unit volume, this term can be written as follows:

$$J_{str} = \beta_s \sum_{i=1}^{N_{ele}} A_i \cdot L_i \quad (9)$$

where β_s is the cost of steel per unit volume, A_i and L_i are the cross-section area and length of the i^{th} element, respectively.

While (J_{damp}) is related to the manufacturing cost of the FVDs. The manufacturing cost of a single damper is correlated to the peak stroke and the square root of the peak force. Since the inter-story drifts are constrained to allowable values, the peak stroke is also limited. For this reason, the peak stroke is not



considered herein as a component of the manufacturing cost of the FVDs. As a result, in this work, the FVDs cost is comprised only of the square root of the peak force of the most loaded damper of each size-group and the number of dampers in that group. The FVDs cost component can be written in the following form:

$$J_{damp} = \beta_d \cdot \left[N_d^{g1} \cdot \sqrt{\max|\hat{\mathbf{f}}_d^{g1}|} + N_d^{g2} \cdot \sqrt{\max|\hat{\mathbf{f}}_d^{g2}|} \right] \quad (10)$$

where β_d is correlated between the peak forces and the cost of the dampers, with the following units $\left(\frac{\text{cost}}{\sqrt{kN}}\right)$. N_d^{g1} and N_d^{g2} are the number of dampers at group one and two, respectively. $\hat{\mathbf{f}}_d^{g1}$ and $\hat{\mathbf{f}}_d^{g2}$ are vectors containing the peak forces developed at each damper that belongs to group one or two, respectively.

3.3 Constraints

In this study, the peak inter-story drift is adopted as the engineering demand parameter (EDP). The inter-story drift is a common criterion to evaluate both the structural and nonstructural damage. For this reason, the inter-story drift should be limited, in order to obtain the desired performance level. This constraint is mathematically formulated in the following form:

$$d_{c,k} = \max_t \left(\left| \frac{d_k(t)}{d_{all}} \right| \right) \leq 1 \quad \forall k = 1 \dots N_{drift} \quad (11)$$

where $d_{c,k}$ is the peak inter-story drift of the k^{th} story, $d_k(t)$ is the inter-story drift of the k^{th} story at time t and d_{all} is the allowable inter-story drift.

The load combination used to evaluate the seismic performance level is based on the EC8 [27] as follows:

$$S_d = 1.0 \cdot D + \psi \cdot L + S_E \quad (12)$$

where D and L represent the dead and the live loads, respectively. S_E is the seismic excitation and ψ is the combination coefficient for the quasi-permanent value of the variable action.

According to the ASCE 7-16 [28], in the case of a structure with added damping, the seismic base shear used for the design of the seismic force-resisting system shall not be less than V_{min} . Where V_{min} is $0.75 \cdot V$ for regular structures and $1.0 \cdot V$ for irregularity structures. Here V is the seismic base shear equal to $V = C_s \cdot W$. Where C_s is the seismic response coefficient and W is the effective seismic weight. This constraint can be written as follows:

$$V_{F.R} \geq V_{min} \quad (13)$$

where $V_{F.R}$ is the seismic lateral force resisting system base shear capacity. Where the capacity is checked by the equivalent lateral procedure (ELF).

In some cases, second order ($P - \Delta$) effects can be a governing criterion in the seismic design of structures. Specially for flexible structures, such as steel MRF, the minimum size of some elements may be determined due to stability consideration. For a single degree of freedom, the stability coefficient is given by:

$$\theta = \frac{P \cdot \delta}{V \cdot h} = \frac{P}{K \cdot h} = \frac{K_G}{K} \quad (14)$$

where P is the total vertical force, δ is the inter story drift, V is the base shear, h is the height of the story, K and K_G are the horizontal stiffness and the geometrical negative stiffness, respectively.

For MDOF structures the stability coefficient can be determined by the following eigenvalue problem, as presented by Bernal [29]:



$$[\mathbf{K} - \lambda_s \mathbf{K}_G] \boldsymbol{\phi}_s = \mathbf{0} \quad (15)$$

where \mathbf{K} and \mathbf{K}_G are the matrix form of K and K_G , respectively. The first eigenvalue $\lambda_{s,1}$ is given as follows:

$$\lambda_{s,1} = \frac{1}{\theta} = \frac{\boldsymbol{\phi}_{s,1}^T \mathbf{K} \boldsymbol{\phi}_{s,1}}{\boldsymbol{\phi}_{s,1}^T \mathbf{K}_G \boldsymbol{\phi}_{s,1}} \quad (16)$$

where $\boldsymbol{\phi}_{s,1}$ is the first mode shape. And finally, the stability coefficient constraint can be formulated as follows:

$$\theta \leq \theta_{max} \quad (17)$$

where θ_{max} is predefined as the maximum value of the stability coefficient determined by code requirements (e.g. 0.1).

In this work, in addition to the seismic design case, a gravity load combination is also considered. Each design checked for gravity load, the gravity design load combination we considered can be written as follows:

$$S_d = 1.5 \cdot D + 1.35 \cdot L \quad (18)$$

Under this load combination, the moment capacity of each member is required to be larger than the design moment. This constraint can be written in the following form:

$$M_y \geq M_d^{gr} \quad \forall j = 1 \dots N_{sec} \quad (19)$$

Another two constraints considered in this work are the “strong column weak beam” and the continuity of the columns at each splice. The “strong column weak beam” requirement appears in most of the modern codes as part of the capacity design philosophy [30,31]. The reason for this constraint is to prevent unwanted soft-story failure mode and increase the chance to achieve the desired global mechanism characterized by plastic hinges at the beam ends. This criterion can be written for each joint as follows:

$$\sum M_{y,c} \geq \gamma \cdot \sum M_{y,g} \quad \forall k = 1 \dots N_{joints} \quad (20)$$

where $\sum M_c$ and $\sum M_g$ are the sums of the yielding moments of all the columns and beams connected to the same joint, respectively and γ is the beam overstrength factor (e.g. 1.2).

The column continuity constraint does not appear in codes. However, many practicing engineers would not welcome a design with a bigger column at the top of the splice in compare to the bottom one. Formally, this constraint is given for each column splice as follows:

$$A_{down}^c \geq A_{up}^c \quad \forall l = 1 \dots N_{splices} \quad (21)$$

where A_{down}^c and A_{up}^c are the cross-section areas of the bottom and top parts of the connected column, respectively.

3.4 Formal optimization scheme – mixed integer form:

Summarizing the components of the problem described above, the formal optimization problem is given as follows:

$$\begin{aligned} & \min_{W, c_d, \gamma_1, \gamma_2} J = J_{str} + J_{damp} \\ & s.t.: \\ & d_{c,k} = \max_t \left(\left| \frac{d_k(t)}{d_{all}} \right| \right) \leq 1 \quad \forall k = 1 \dots N_{drift} \\ & V_{F.R} \geq V_{min} \end{aligned} \quad (22)$$



$$\begin{aligned}
 M_y &\geq M_d^{gr} & \forall j = 1 \dots N_{sec} \\
 \sum M_c &\geq \gamma \cdot \sum M_g & \forall k = 1 \dots N_{joints} \\
 A_{down}^c &\geq A_{up}^c & \forall l = 1 \dots N_{spllices} \\
 \theta &\leq \theta_{min} \\
 y_2 &\geq y_1
 \end{aligned}$$

(22 Cont.)

With:

$$\begin{aligned}
 \mathbf{M}\ddot{\mathbf{u}}(t) + \mathbf{C}_s\dot{\mathbf{u}}(t) + \mathbf{f}_s(t) + \mathbf{f}_d(t) &= -\mathbf{M}\mathbf{e}\mathbf{a}_g(t) ; \forall \mathbf{a}_g(t) \in \varepsilon \\
 \mathbf{u}(0) = \mathbf{u}_{static}, \dot{\mathbf{u}}(0) = \mathbf{0}, \mathbf{f}_s(0) = \mathbf{f}_{s,static}, \mathbf{f}_d(0) &= \mathbf{0} \\
 [\mathbf{K} - \lambda_s \mathbf{K}_G] \boldsymbol{\phi}_s &= \mathbf{0} \\
 \mathbf{K}\mathbf{u} &= \mathbf{F}_{ELF} \\
 \mathbf{K}\mathbf{u} &= \mathbf{F}_{gravity} \\
 W_i &\in \{W_1, W_2, W_3, \dots\} \\
 c_{d,j} &\in \{0, \bar{c}_d \cdot y_1, \bar{c}_d \cdot y_2\}
 \end{aligned}$$

The optimization problem presented in (22) is solved by Genetic Algorithm (GA). The numerical results are given in section 4.

4. Numerical Example

This section presents how the new problem formulation given in (22) successfully leads to a practical and optimized solution. As described in previous sections, the proposed method relies on standard cross-sections and is limited to two size-groups for the FVDs. The total cost of the structural elements and the dampers is optimized, while the constraints are satisfied.

For the numerical example, we consider a 2-D five-story steel frame (Fig. 4) to be optimized. The frame is subjected to the LA02 ground record from the LA 10% @ 50 years ensemble. The ground acceleration as a function of time is given in Fig. 3. We consider the Rayleigh inherent damping matrix based on 5% of critical damping for the first and the third modes. The sections of the columns and beams are selected out of the HEB and IPE steel tables, respectively. A dead load of $D = 3 \left[\frac{kN}{m^2} \right]$, live load of $L = 5 \left[\frac{kN}{m^2} \right]$ and $\psi = 0.3$ were considered. The yield stresses of the columns and beams elements are 345 [Mpa] and 248 [Mpa], respectively. The ground structure considered in this example is shown in Fig. 4b. Fourteen types of elements (four columns and ten beams) and ten possible locations for the FVDs (two at each bay) are all to be optimized. Each element is selected out of seven options (HEB 260-400 for the columns and IPE 270-500 for the beams). The parameters of the dampers are determined as follows: $\bar{c}_d = 100 \left[kN \left(\frac{sec}{mm} \right)^\alpha \right]$, $K_{eq,j} = 2 \cdot c_{d,j} \left[\frac{kN}{mm} \right]$. Nonlinear dampers with an exponent of $\alpha = 0.35$ are considered. The objective function is evaluated based on $\beta_s = 39,250 \left(\frac{\$}{m^3} \right)$ which corresponds with $5,000 \left(\frac{\$}{ton} \right)$ for the steel price. For the dampers price the parameter β_d is set to $447 \left(\frac{\$}{\sqrt{kN}} \right)$, based on the practical price of 10,000\$ for a damper defined by a force capacity of 500 [kN]. The minimum allowed value for the stability coefficient is $\theta_{min} = 0.1$. The force-resisting system is designed for a minimum base shear of $V_{min} = 645.6 [kN]$ and the overstrength factor for the “strong column weak beam” constraint is set to $\gamma = 1.2$.

The optimization process is carried on using the MATLAB built-in Genetic Algorithm function. A number of stopping criteria are set. Among the criteria: maximum number of generations, if the average relative change in the best fitness function value over “MaxStallGenerations” is less than or equal to “FunctionTolerance”. For numerical experiments a parallel-processor MATLAB code was executed on Tamnun, a computer cluster hosted and maintained by the Division for Computing and Information System at the Technion–Israel Institute of Technology.



To reduce the computational effort each design is first checked against all the constraints except the performance constraint. Only the designs that satisfy these constraints are further evaluated to check whether they satisfy the drifts constraint. Evaluating this constraint requires a computationally consuming NRHA that is avoided if other constraints are not satisfied.

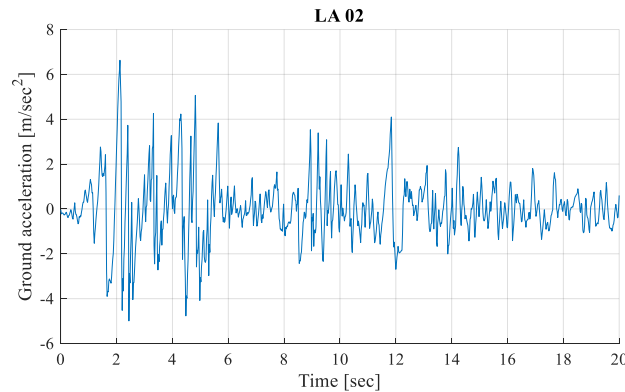


Fig. 3 – LA02 ground record

In this section, the structure presented in Fig. 4 is to be optimized. Two cases are considered herein. First, the frame is designed for a high-performance level, characterized by an inter-story drift of 1% of the story height. In the second case, the same frame is designed for a standard performance level, characterized by an inter-story drift of 2% of the story height.

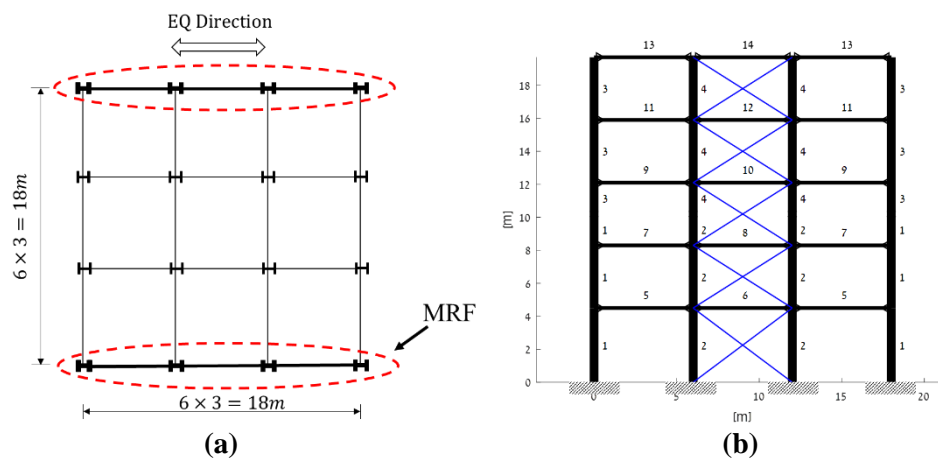


Fig. 4 – plan view (a); elevation view of the MRF (b)

4.1 High performance level

The GA parameters were determined as follows: the maximum number of generations is set to 200; MaxStallGenerations=20 and FunctionTolerance=1E-6.

The optimal design has been obtained after 94 generations; the optimal layout of the frame is shown in Fig. 5(a). The two groups of dampers are marked in blue and red, the group defined by the larger damping coefficient $c_{d,1} = 35 \left[kN \left(\frac{sec}{mm} \right)^\alpha \right]$ is in red and the other group with the smaller damping coefficient $c_{d,2} = 34 \left[kN \left(\frac{sec}{mm} \right)^\alpha \right]$ is in blue. The thickness of the frame elements in Fig. 5(a) represent the cross-section properties of each one of them. The normalized pack inter-story drifts of the different stores are given in Fig. 5(b). As can be seen, the peak inter-story drifts of all five stories are relatively close to the predefined allowable values.

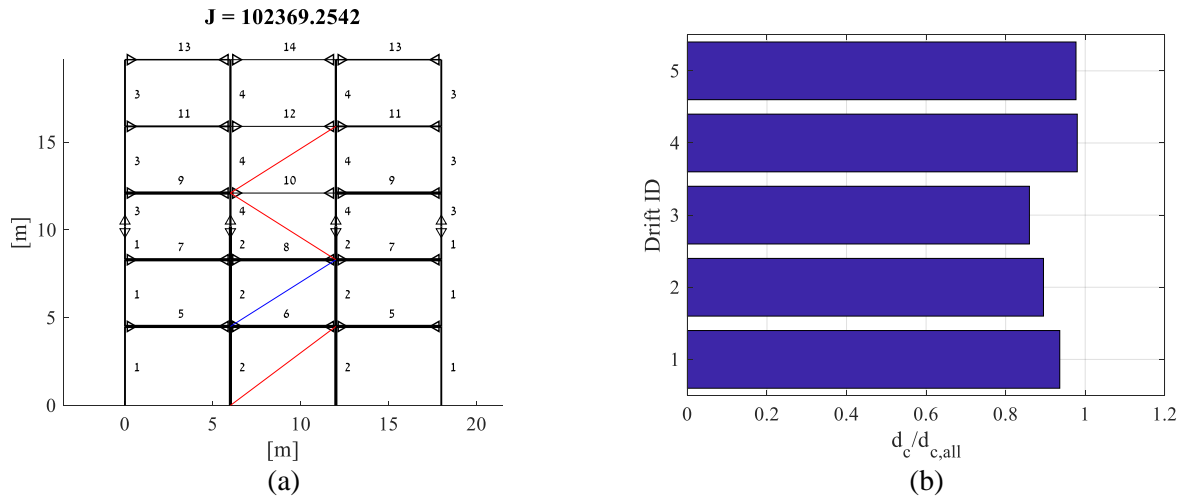


Fig. 5 – optimized structure (a) normalized inter-story drifts (b)

4.2 Standard performance level

The optimization process stopped after 54 generations, the optimal layout of the frame is shown in Fig. 6(a) in this case the optimal solution relies on the force resisting system alone. The thickness of the frame elements in Fig. 6(a) represent the cross-section properties of each one of them. The normalized peak inter-story drift of the different stories is given in Fig. 6(b).

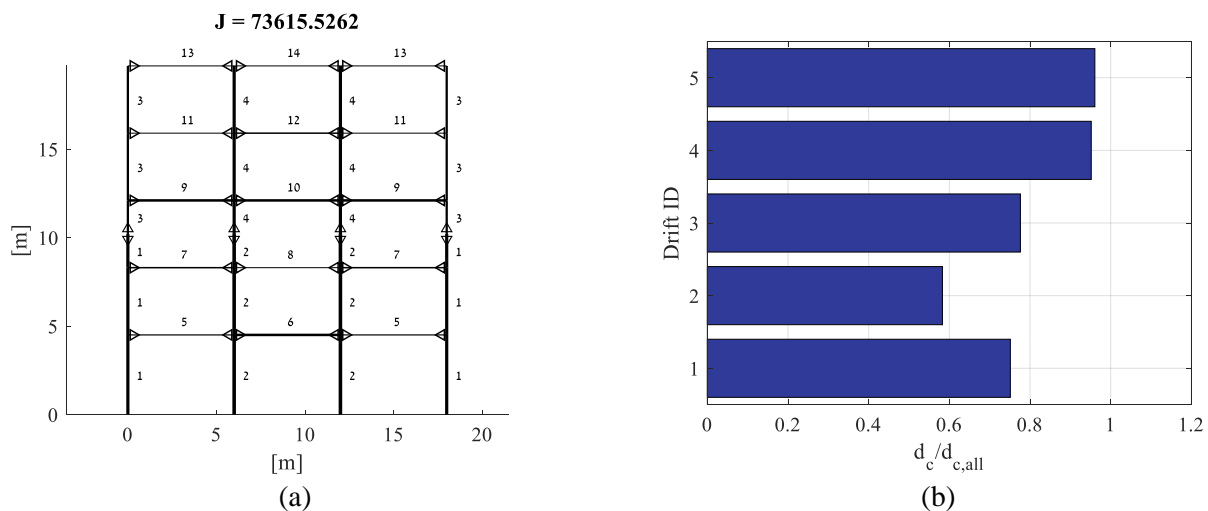


Fig. 6 – optimized structure (a) normalized peak inter-story drifts (b)

Table 1 shows the main differences between the optimized results based on the two different performance levels.

Table 1 – Comparison between the two performance levels

	Peak drift /allowable drift	$V_{min}/V_{F.R}$	θ/θ_{min}	M_d^{gr}/M_y	$J = J_{str} + J_{damp}$
High performance level	98%	89%	40%	87%	$102,369=73,526+28,843$
Standard performance level	96%	99%	43%	89%	$73,616=73,616+0$



5. Conclusions

In this paper, a problem formulation for the optimal design of both the structural elements and the properties (locations and sizes) of FVDs was presented. The formulation considered the cross-sections and FVDs properties as design variables through the optimization process. Therefore, a large design space that includes the dampers and elements is explored and more efficient design may be reached. The goal of the optimization is to minimize the combined cost of the steel elements and FVDs, while several constraints are satisfied. The framework accounting for a number of codes constrains beside a performance constraint. As part of the proposed formulation, the structural response is evaluated based on NRHA. The NRHA relies on a spread plasticity beam model and the Maxwell model for the nonlinear FVDs. The problem is solved using GA.

The numerical results demonstrated the strength of the proposed formulation to achieve solutions that simultaneously optimize the cross-sections and the FVDs properties. Two performance levels were considered and compared, the methodology attained a design with FVDs for the high-performance level, while for the standard performance level the optimized structure relies on the conventional resisting system alone.

6. References

- [1] Ganzerli, S., Pantelides, C.P. and Reaveley, L.D. (2000) Performance-based design using structural optimization. *Earthquake Engineering and Structural Dynamics*, **29**, 1677–90. [https://doi.org/10.1002/1096-9845\(200011\)29:11<1677::AID-EQE986>3.0.CO;2-N](https://doi.org/10.1002/1096-9845(200011)29:11<1677::AID-EQE986>3.0.CO;2-N)
- [2] Chan, C.M. and Zou, X.K. (2004) Elastic and inelastic drift performance optimization for reinforced concrete buildings under earthquake loads. *Earthquake Engineering and Structural Dynamics*, **33**, 929–50. <https://doi.org/10.1002/eqe.385>
- [3] Zou, X. K., Chan, C.M. (2005) An optimal resizing technique for seismic drift design of concrete buildings subjected to response spectrum and time history loadings. *Computers & structures, . Engineering Structures*, **27**, 1689-1704. <https://doi.org/10.1016/j.engstruct.2005.04.001>
- [4] Fragiadakis, M. and Papadrakakis, M. (2008) Performance-based optimum seismic design of reinforced concrete structures. *Earthquake Engineering and Structural Dynamics*, **37**, 825–44. <https://doi.org/10.1002/eqe.786>
- [5] Lavan, O. and Wilkinson, P.J. (2016) Efficient Seismic Design of 3D Asymmetric and Setback RC Frame Buildings for Drift and Strain Limitation. *Journal of Structural Engineering*, 04016205. [https://doi.org/10.1061/\(ASCE\)ST.1943-541X.0001689](https://doi.org/10.1061/(ASCE)ST.1943-541X.0001689)
- [6] Liu, M., Burns, S.A. and Wen, Y.K. (2005) Multiobjective optimization for performance-based seismic design of steel moment frame structures. *Earthquake Engineering and Structural Dynamics*, **34**, 289–306. <https://doi.org/10.1002/eqe.426>
- [7] Fragiadakis, M. and Lagaros, N.D. (2011) An overview to structural seismic design optimisation frameworks. *Computers and Structures*, Elsevier Ltd. **89**, 1155–65. <https://doi.org/10.1016/j.compstruc.2010.10.021>
- [8] Lagaros, N.D., Fragiadakis, M., Papadrakakis, M. and Tsompanakis, Y. (2006) Structural optimization: A tool for evaluating seismic design procedures. *Engineering Structures*, **28**, 1623–33. <https://doi.org/10.1016/j.engstruct.2006.02.014>
- [9] Lavan, O. and Levy, R. (2010) Performance based optimal seismic retrofitting of yielding plane frames using added viscous damping. *Earthquake and Structures*, **1**, 307–26. <https://doi.org/10.12989/eas.2010.1.3.307>
- [10] Pollini, N., Lavan, O. and Amir, O. (2016) Towards realistic minimum-cost optimization of viscous fluid dampers for seismic retrofitting. *Bulletin of Earthquake Engineering*, **14**, 971–98. <https://doi.org/10.1007/s10518-015-9844-9>
- [11] Takewaki, I. (1997) Optimal Damper Placement for Minimum Transfer. **26**, 1113–24.
- [12] Gluck, N., Reinhorn, A.M., Gluck, J. and Levy, R. (1996) Design of supplemental dampers for control of structures. *J. Struct. Eng.* p. 1394–9. [https://doi.org/10.1061/\(ASCE\)0733-9445\(1996\)122:12\(1394\)](https://doi.org/10.1061/(ASCE)0733-9445(1996)122:12(1394))



- [13] Lopez Garcia, D. and Soong, T.T. (2002) Efficiency of a simple approach to damper allocation in MDOF structures. *Journal of Structural Control*, **9**, 19–30. <https://doi.org/10.1002/stc.3>
- [14] Singh, M.P. and Moreschi, L.M. (2002) Optimal placement of dampers for passive response control. *Earthquake Engineering and Structural Dynamics*, **31**, 955–76. <https://doi.org/10.1002/eqe.132>
- [15] Kanno, Y. (2012) Damper Placement Optimization in a Shear Building Model with Discrete Design Variables : A Mixed-Integer Second-Order Cone Programming Approach.
- [16] Viti, S., Cimellaro, G.P. and Reinhorn, A.M. (2006) Retrofit of a hospital through strength reduction and enhanced damping. *Smart Structures and Systems*, **2**, 339–55. <https://doi.org/10.12989/sss.2006.2.4.339>
- [17] Takewaki, I. (1999) Displacement-acceleration control via stiffness-damping collaboration. *Earthquake Engineering and Structural Dynamics*, **28**, 1567–85. [https://doi.org/10.1002/\(SICI\)1096-9845\(199912\)28:12<1567::AID-EQE882>3.0.CO;2-1](https://doi.org/10.1002/(SICI)1096-9845(199912)28:12<1567::AID-EQE882>3.0.CO;2-1)
- [18] Cimellaro, G.P. (2007) Simultaneous stiffness-damping optimization of structures with respect to acceleration, displacement and base shear. *Engineering Structures*, **29**, 2853–70. <https://doi.org/10.1016/j.engstruct.2007.01.001>
- [19] Lavan, O., Cimellaro, G.P., Asce, M., Reinhorn, A.M. and Asce, F. (2008) Noniterative Optimization Procedure for Seismic Weakening. **134**, 1638–48. [https://doi.org/10.1061/\(ASCE\)0733-9445\(2008\)134](https://doi.org/10.1061/(ASCE)0733-9445(2008)134)
- [20] Lavan, O. (2015) A methodology for the integrated seismic design of nonlinear buildings with supplemental damping. *Structural Control and Health Monitoring*, **22**:484–499. <https://doi.org/10.1002/stc>
- [21] Oohara, K., & Kasai, K. (2002) Time-history analysis model for nonlinear viscous dampers. In Structural engineers world congress (SEWC). Yokohama, Japan..
- [22] Spacone, E., Ciampi, V. and Filippou, F.C. (1996) Mixed formulation of nonlinear beam finite element. *Computers and Structures*, **58**, 71–83. [https://doi.org/10.1016/0045-7949\(95\)00103-N](https://doi.org/10.1016/0045-7949(95)00103-N)
- [23] Sivaselvan, M. V. and Reinhorn, A.M. (1999) Hysteretic Models for Cyclic Behavior of Deteriorating Inelastic Structures. *Technical Report NCEER-99-0018, National Center for Earthquake Engineering Research, State University of New York at Buffalo*,.
- [24] Pollini, N., Lavan, O. and Amir, O. (2018) Optimization-based minimum-cost seismic retrofitting of hysteretic frames with nonlinear fluid viscous dampers. *Earthquake Engineering and Structural Dynamics*, **47**, 2985–3005. <https://doi.org/10.1002/eqe.3118>
- [25] Rutenberg, A. (1981) A direct P-delta analysis using standard plane frame computer programs. *Computers & Structures*, **14**, 97–102.
- [26] Xu, L., Gong, Y. and Grierson, D.E. (2006) Seismic design optimization of steel building frameworks. *Journal of Structural Engineering*, **132**, 277–86. [https://doi.org/10.1061/\(ASCE\)0733-9445\(2006\)132:2\(277\)](https://doi.org/10.1061/(ASCE)0733-9445(2006)132:2(277))
- [27] Eurocode 8.(2004). “Design provisions for earthquake resistant structures”. CENENV.
- [28] ASCE/SEI (ASCE/Structural Engineering Institute). (2016). “Minimum design loads for buildings and other structures.” ASCE/SEI 7-16, Reston, VA.
- [29] Bernal, D. (1998) Instability of buildings during seismic response. *Engineering Structures*, **20**, 496–502. [https://doi.org/10.1016/S0141-0296\(97\)00037-0](https://doi.org/10.1016/S0141-0296(97)00037-0)
- [30] Hollings, J. (1969) Reinforced concrete seismic design. *Bull New Zealand Soc Earthq Eng*, **2(3):217-2**.
- [31] Park, R. and Paulay, T. (1975) Reinforced Concrete Structures. Wiley, **New York**,.